International Journal of
Molecular Sciences

MDPI

Article

Antioxidant Potential of Aqueous Dispersions of Fullerenes C_{60}, C_{70}, and $Gd@C_{82}$

Ivan V. Mikheev [1,*], Madina M. Sozarukova [1,2], Dmitry Yu. Izmailov [3], Ivan E. Kareev [4], Elena V. Proskurnina [5] and Mikhail A. Proskurnin [1]

1 Analytical Chemistry Division, Chemistry Department, Lomonosov Moscow State University, 119991 Moscow, Russia; s_madinam@bk.ru (M.M.S.); proskurnin@gmail.com (M.A.P.)
2 Kurnakov Institute of General and Inorganic Chemistry, Russian Academy of Sciences, 119991 Moscow, Russia
3 Faculty of Fundamental Medicine, Lomonosov Moscow State University, 119234 Moscow, Russia; dizm@mail.ru
4 Institute of Problems of Chemical Physics of the Russian Academy of Sciences, 142432 Moscow, Russia; kareev@icp.ac.ru
5 Research Centre for Medical Genetics, 115522 Moscow, Russia; proskurnina@gmail.com
* Correspondence: mikheev.ivan@gmail.com; Tel.: +7-(495)-939-1568 (ext. 101)

Abstract: The antioxidant potential (capacity and activity) of aqueous fullerene dispersions (AFD) of non-functionalized C_{60}, C_{70}, and $Gd@C_{82}$ endofullerene (in micromolar concentration range) was estimated based on chemiluminescence measurements of the model of luminol and generation of organic radicals by 2,2′-azobis(2-amidinopropane) dihydrochloride (ABAP). The antioxidant capacity was estimated by the TRAP method, from the concentration of half-suppression, and from the suppression area in the initial period. All three approaches agree and show that the antioxidant capacity of AFDs increased in the order $Gd@C_{82} < C_{70} < C_{60}$. Mathematical modeling of the long-term kinetics data was used for antioxidant activity estimation. The effect of C_{60} and C_{70} is found to be quenching of the excited product of luminol with ABAP-generated radical and not an actual antioxidant effect; quenching constants differ insignificantly. Apart from quenching with a similar constant, the AFD of $Gd@C_{82}$ exhibits actual antioxidant action. The antioxidant activity in $Gd@C_{82}$ is 300-fold higher than quenching constants.

Keywords: fullerene; endofullerene; aqueous fullerene dispersion; antioxidant capacity; antioxidant activity; chemiluminometry

Citation: Mikheev, I.V.; Sozarukova, M.M.; Izmailov, D.Y..; Kareev, I.E.; Proskurnina, E.V.; Proskurnin, M.A. Antioxidant Potential of Aqueous Dispersions of Fullerenes C_{60}, C_{70}, and $Gd@C_{82}$. *Int. J. Mol. Sci.* **2021**, *22*, 5838. https://doi.org/10.3390/ijms22115838

Academic Editors: Taku Shoji and Tetsuo Okujima

Received: 29 April 2021
Accepted: 27 May 2021
Published: 29 May 2021

1. Introduction

Water-soluble fullerene species are promising for various medical applications, and they have been proposed as vital components for humans and environmental systems [1]. Fullerenes and, in particular, their water-soluble derivatives, are considered radical scavenging agents [2], possess antioxidant activity [3], acquire remarkable antimicrobial properties [4], cytotoxicity [5], DNA cleavage, and lipid peroxidation mediated by reactive oxygen species (ROS) [6].

The investigation of non-functionalized (without addends) aqueous fullerene dispersions (AFD), which are produced by ultrasound-assisted solvent exchange [7], dialysis [8], or direct ultrasonic treatment [9], is developing widely. The mechanism of AFD stabilization is not fully understood, but attempts have been made to explain it by hydroxylation of the fullerene cage [10]. Recently, substantial advances have been made in areas of colloidal fullerene properties [11], physicochemical interactions at the nano–bio interface [12], biological mechanisms and physicochemical characteristics responsible for driving fullerene toxicity [13], and biological activity of water-soluble fullerene adducts [14].

The recent review discussed [15] that fullerenes possess an inert scaffold with antioxidant functionalities. C_{60} is a very weak chain-breaking antioxidant with an inherent rate

constant for trapping peroxyl radicals per se (k_{inh}=0.3 × 10^3 M^{-1} s^{-1}). However, some antioxidants covalently bound to fullerenes increase antioxidant activity insignificantly. Grafting their cage with small-molecule antioxidant moieties such as synthetic phenols (2,6-di-tert-butyl-4-methylphenol) broadens their antioxidant potential conveying peroxyl radical-trapping activity up to 30 times [16]. C_{60} conjugated with phenols indicates a significant improvement of oxidative stability [17]. A C_{60} derivative with covalently bonded analog of α-tocopherol with hydroxychromanyl moiety is an effective antioxidant acting in model lipid matrices: saturated stearic acid and unsaturated linolenic acid during the non-isothermal oxidation tested by differential scanning calorimetry [18].

Derivatives $C_{60}(C(COOH)_2)_2$, $C_{60}(OH)_{22}$, and $Gd@C_{82}(OH)_{22}$ can stabilize the mitochondrial membrane potential and reduce intracellular ROS production in the order: $Gd@C_{82}(OH)_{22} \geq C_{60}(OH)_{22} > C_{60}(C(COOH)_2)_2$. These derivatives scavenge the stable 2,2-diphenyl-1-picryhydrazyl radical, ROS, and inhibit lipid peroxidation in vitro [19]. The common fullerene derivatives in the structure are fullerenols, with up to 42 hydroxyl groups, depending on the fullerene type. Hydroxylation is one of the cheapest and most straightforward approaches to dissolving fullerenes in water and does not require deep purification of the resulting product. However, even minor surface derivatization may increase the antioxidant activity of fullerenes [20]. Less toxicity and greater antioxidant capacity are proven for fullerenols $C_{60}O_y(OH)_x$, $C_{60,70}O_y(OH)_x$, x + y = 24 ÷ 28 [21]. There are two limitations of any derivatization of fullerene cage. First, these groups can be involved in metabolic processes; they can reduce the π-electron system availability leading to reversible free radical capture [22], differently affecting the spin environment [23]. Second, fullerene derivatives could act as potent oxidizing agents under excitation with light in the presence of oxygen [24].

The radical reactivity of fullerenes is discussed [25]. First attempts at studying superoxide dismutase (SOD) mimic activity have yet to be made [26] for in vitro and cell models. It is known that unsaturated lipids are a target of free radicals. Their oxidation (lipid peroxidation) mechanism has been described and proven [6]. The result is the accumulation of lipid hydroperoxides as intermediate stable products. The ability of fullerenes to initiate lipid oxidation has not been widely assessed. There is a report on their ability to trap lipid peroxyl radicals and act as chain-breaking antioxidants [27]. The impact of fullerenes in in vivo and in vitro experiments for *Cyprinus carpio* brains confirmed the absence of lipid peroxidation [28]. The protective action of C_{60} most probably results from its ability to be included in the cell membrane and avoid lipid peroxidation [29].

The antioxidant and superoxide anion-radical (SAR) scavenging properties of non-functionalized AFDs have not been thoroughly studied [30]. The data on the antioxidant activity of unmodified fullerenes in their aqueous dispersions are almost absent. There is an ambiguity in the information about the ability of fullerenes to generate ROS. Several studies deal with C_{60} solutions stimulating ROS generation [31]. Another study evidenced the antioxidative properties of fullerenes [32]. Additionally, the possible antioxidant mechanism of fullerenes, in particular C_{60}, deals with loading their molecules with protons to acquire a positive charge distributed over the fullerene. Such charge-loaded particles could be transferred through the inner membrane of mitochondria. In this case, the transmembrane potential is reduced [33], significantly reducing SAR production [34]. Furthermore, C_{60} is capable of penetrating an artificial lipid bilayer [35]. Fullerene soot C_{60} and C_{70} not only retards oxidation as an alkyl radical quencher but also operates as a peroxy radical scavenger [36] in the model reaction of initiated (2,2′-azobisisobutyronitrile, AIBN). For reactivity of C_{60} during oxidation of a series of hydrocarbons shows that the fullerene does not react with the $RO_2^{\bullet}$ radicals indicate an extremely weak rate constant estimated from CL [37].

The conventional approach to describing the antioxidant properties of low molecular weight free-radical scavengers is based on a quantitative assessment of their ability to terminate free-radical chain reactions against a standard antioxidant compound. Evaluation of the antioxidant status of compounds, the total radical-trapping potential (TRAP)

method, and total antioxidant reactivity (TAR) from luminol-enhanced chemiluminescence (CL) measurements have been previously developed [38]. This approach is based on the ability to trap radicals formed during the decomposition of thermolabile azo compounds. However, this technique does not consider the physicochemical parameters of the antioxidant. A more rigorous approach to the description of antioxidant properties considers the determination of the antioxidant concentration and the mathematical modeling [39] of the rate constant of the interaction with the radicals [40]. Different antioxidants result in different chemiluminescence curves, making it impossible to use any single parameter to characterize the activity of substances of different chemical nature [41].

The antioxidant potential is an umbrella term to quantitatively describe the thermodynamic and kinetic aspects of the antioxidant action [42]. In this work, we assessed both the thermodynamic *antioxidant capacity* (the total number of neutralized radicals per unit of fullerene concentration) by quantitative comparison with Trolox® as a reference compound [38]. We also applied mathematical modeling to estimate rate constants of fullerenes, i.e., the kinetic *antioxidant activity* (the dynamic interception ability of radicals) [39]. As far as we are concerned, kinetics modeling for fullerenes were not used previously.

Thus, this paper deals with the antioxidant potential of aqueous fullerene dispersions of C_{60}, C_{70}, and Gd@C_{82} as both antioxidant capacity and antioxidant activity using various approaches, including computer simulation. The antioxidant potential of AFDs was estimated using luminol-enhanced chemiluminescence with 2,2′-azobis(2-amidinopropane) dihydrochloride (ABAP, 2.5 mM) as a source of free radicals at 37 °C in a phosphate buffer solution (100 mM, pH 7.4).

2. Results

2.1. Assessment of the Antioxidant Capacity of AFDs

Here, the "antioxidant potential" means both antioxidant activity and antioxidant capacity. In the technical IUPAC report [43], the terms "antioxidant capacity/activity" have not been separated, although these parameters are rather complementary. The antioxidant capacity (the number of neutralized radicals per unit of fullerene concentration) was assessed using the modified TRAP protocol [44] and TAR protocol [38]. The TRAP index is calculated from the latent period (Figure 1), while the TAR index is obtained from the rapid decrease in luminescence after adding the antioxidant. The antioxidant activity (kinetic constants of the reaction of an antioxidant with a free radical) has been determined using the computer simulation of the chemiluminescence kinetics.

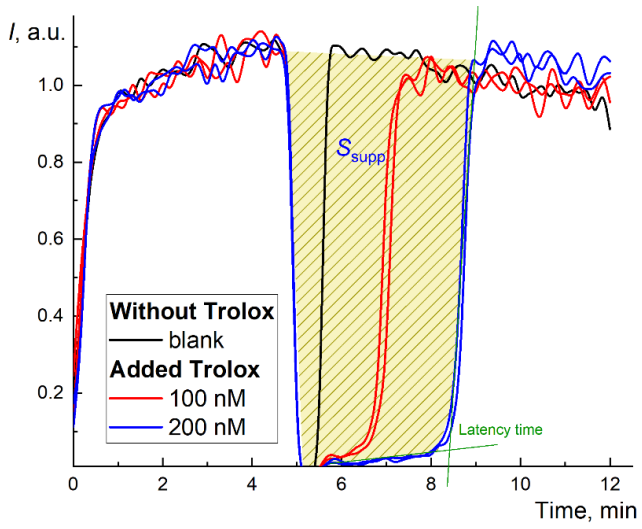

Figure 1. Long-term chemiluminograms of a strong antioxidant Trolox® in the system 2.5 mM ABAP and 2 μM luminol up to 100 min. The figure shows the latency period and the principle of calculating the area of signal suppression (for the concentration of 200 nM, blue line).

In the TRAP method, Trolox is used as a reference substance [45]. The chemiluminograms for Trolox (100 and 200 nM) are shown in Figure 1. The effect of Trolox in the ABAP/luminol system is typical for strong antioxidants: the complete suppression of chemiluminescence followed by complete depletion of the antioxidant with a rapid increase in the CL intensity to the previous stationary (blank) level after the latent period [46]. However, the latent period depends on the initial stationary CL level I_0 and requires precise measurements of a short suppression period and restoration of the level I_0 after the antioxidant action. Thus, it provides reliable data for strong antioxidants only.

Therefore, to assess the antioxidant capacity by an alternative approach, we used the area of suppression of chemiluminescence S (Figure 1), which is proportional to the total number of radicals scavenged by the antioxidant, i.e., antioxidant capacity. The kinetics of the antioxidant action for fullerenes differed from Trolox (Figure 2a,c,e). Instead of almost rectangular ("trough") suppression of the signal (Figure 1), we observed a decrease in the stationary level typical for "weak" (or relatively slow) antioxidants. Strictly speaking, it was not possible to wait until the signal returned to the stationary level for all three fullerenes (i.e., the antioxidant was consumed, Figure 2b,d,f).

However, we estimated the area of signal suppression S_{supp} for C_{60} and C_{70} (shaded areas in Figure 2b,d; for $Gd@C_{82}$, we failed to calculate this area correctly as the antioxidant was not consumed during the operation of the CL model, and the CL intensity did not return to the initial level. The integration suppression area normalized to concentration (Table 1) showed the behavior, $C_{60} > C_{70} > Gd@C_{82}$, ratios 4.3:2.4:1. The recalculation of S_{supp} to Trolox showed C_{60} has a 3-fold lower capacity than Trolox and $Gd@C_{82}$, at 7% capacity compared to Trolox.

Table 1. Antioxidant capacity parameters for aqueous fullerene dispersions: area of suppression of the chemiluminescence signal (Ss_{upp}) normalized to 1 μM of AFDs; Trolox equivalents calculated for 1 μM of AFDs; area of suppression of the chemiluminescence signal for the first 20 min (S_{20}); and half-maximal inhibitory concentration ($c_{1/2}$); $n = 5$, $p = 0.95$.

AFD	Concentration Range, μM	TRAP		Suppression Area for the First 20 min, Linear Fit	$c_{1/2}$, μM
		Normalized $S_{supp} \times 10^{-6}$	Trolox Equivalent, μM		
C_{60}	1.8 ÷ 18	0.51	0.31	$S_{20} = (76 \pm 6) \times c_{Ful}$, $r = 0.9955$	6.4 ± 0.3
C_{70}	2.0 ÷ 20	0.29	0.18	$S_{20} = (46 \pm 2) \times c_{Ful}$, $r = 0.9956$	11.0 ± 0.4
$Gd@C_{82}$	4.0 ÷ 40	0.12	0.072	$S_{20} = (28 \pm 5) \times c_{Ful}$, $r = 0.9754$	22.6 ± 0.8

As calculating the area of suppression of chemiluminescence was unsuitable for $Gd@C_{82}$, and with some reservations applicable for C_{60} and C_{70}, we used a different method for determining the capacity. The addition of weak antioxidants leads not to the complete suppression but to a decrease in chemiluminescence intensity plateau ΔI. However, the dependence of ΔI on c for fullerenes proved to be nonlinear (Figure 2a,c,e), and the CL intensity does not show a stable plateau. Thus, we used an approach based on the combination of the intensity decrease and the suppression area [44]. We calculated the suppression area for the first 20 min of the reaction, S_{20} (Table 1). This value for low antioxidant capacities is more accurate than TRAP or TAR because the results do not depend on the initial level of chemiluminescence [44], and thus both high and low antioxidant capacities can be compared [47]. By this approach, AFDs can be ranked as $C_{60} > C_{70} > Gd@C_{82}$ (Table 1), capacity ratios are 2.7:1.6:1.

Furthermore, for weak antioxidants, the antioxidant capacity can be estimated by the concentration of semi-suppression of the initial luminescence ($c_{1/2}$) [21]. By this approach, AFDs can be ranked as $C_{60} > C_{70} > Gd@C_{82}$ (Table 1). Ratios of reciprocal half-suppression signal concentrations were 3.5:1.7:1.

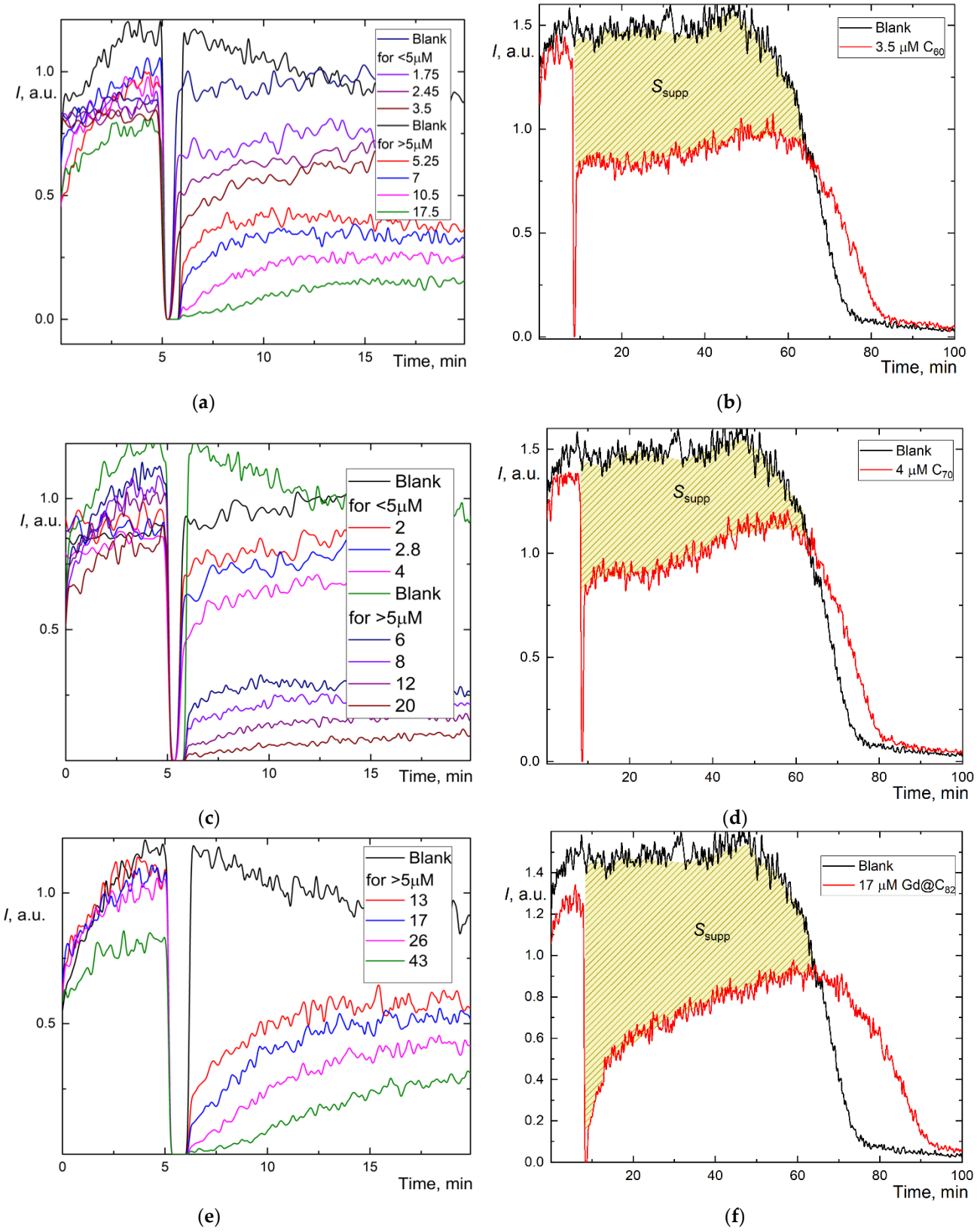

Figure 2. Chemiluminograms of aqueous fullerene dispersions (AFD) in 2.5 mM ABAP and 2 μM luminol (**a**) C_{60} in the concentration range of 1.8–18 μM up to 20 min; (**b**) long-term chemiluminograms of C_{60} (3.5 μM) up to 100 min; (**c**) C_{70} in a range of concentration 2.0–20 μM up to 20 min; (**d**) long-term chemiluminograms of C_{70} (4.0 μM) up to 100 min; (**e**) Gd@C_{82} in a range of concentration 4.0–40 μM; (**f**) long-term chemiluminograms of Gd@C_{82} (17 μM) up to 100 min. A sharp decrease in the signal between 5 and 10 min results from adding AFDs, the signal is not registered.

Thus, the results of estimation by TRAP suppression area, the suppression area for the first 20 min of the reaction, S_{20}, and $c_{1/2}$ agree with each other. These rows are also in accordance with the fraction of active molecules on the surface of fullerene clusters in AFDs, 1.8:1.6:1 [26]. As a whole, the antioxidant capacities of studied fullerenes in AFD by three approaches lie within one order of magnitude, and they show the properties of weak antioxidants.

2.2. Antioxidant Activity (Chemiluminescence Kinetics before Antioxidant Depletion)

A mathematical model simulating the steady-state level of chemiluminescence without antioxidants consisted of two reactions: (1) the free-radical generation from ABAP and (2) chemiluminescence reactions:

1) ABAP $\rightarrow$ R$^\bullet$ (constant k_R), decomposition of ABAP
2) R$^\bullet$ + Lum $\rightarrow$ RLum* (constant k_{Lum}), formation of the excited product
2a) RLum* $\rightarrow$ P + $h\nu$ luminescence

where R$^\bullet$ is a free radical or reaction product in the electronically excited state, which reacts with antioxidants, and P is the stable product of the free-radical reaction.

Fullerenes are known to be both antioxidants [48] and fluorophores [49] and act as fluorescence quenchers [50,51]. We evaluated the properties of fullerenes as quenchers for the ABAP–luminol system (Figures S1 and S2, Supplementary Materials). The Stern–Volmer constants are C_{60}~C_{70} > Gd@C_{82}, (3.7 ± 0.1, 3.8 ± 0.1, and 2.9 ± 0.1) $\times 10^4$ M^{-1}, respectively, which have good accordance with the existing data [32,52,53]. The fluorescence spectra are presented in the Supplementary Materials. From these data, we expected that fullerenes might play two roles in the system: actual antioxidant action and chemiluminescence quenching. Thus, to model the action of AFDs, we took into account the following reactions:

3) AO + R$^\bullet$ $\rightarrow$ ... (antioxidant action, constant k_{In1})
3a) AO + RLum* $\rightarrow$ ... (excited product quenching, constant k_{In2})

Rate constants of the inhibition reactions 3 and 3a are used to prove and estimate the antioxidant activity.

To simulate the reaction kinetics, we recorded the chemiluminograms until complete luminol depletion [44]. All AFDs satisfy the requirements for mathematical modeling: (1) the moment of antioxidant depletion is registered, and (2) the concentration dependence is traced. To carry out the simulation, we selected the optimum concentration ranges of the investigated AFDs (close to $c_{1/2}$; Table 1). The initial simulation conditions are summed up in Table 2. The experimental and model plots for AFD are shown for C_{60} (Figure 3a), C_{70} (Figure 3b), and Gd@C_{82} (Figure 3c).

Table 2. Constants for a one-stage mechanism for C_{60} and C_{70}, and two-stage for Gd@C_{82}. Initial simulation conditions common for all the studied systems: ABAP, 2.5 mM; luminol, 2 μM; radical of ABAP and the excited product area were absent at the starting points.

Initial Concentrations, μM	C_{60}	C_{70}	Gd@C_{82}	Trolox®	Reaction
AO	3.5	4.0	17.2	0, 0.1, and 0.2	Quenching reaction (3a)
AO	n/a	n/a	0.172	n/a	Radical interception reaction (3)
Value of Simulated Constant, μM^{-1} min^{-1}					
ABAP $\rightarrow$ R	1.25			1.70	ABAP decomposition (1)
R + Lum $\rightarrow$ RLum*	2				Formation of an excited product (2)
RLum* $\rightarrow$ P + $h\nu$	1			4	Luminescence (2a)
AO + R$^\bullet$ $\rightarrow$ ...	n/a	n/a	30	10,000	Radical interception reaction (3)
AO + RLum* $\rightarrow$ ...	0.20	0.13	0.13	n/a	Quenching reaction (3a)

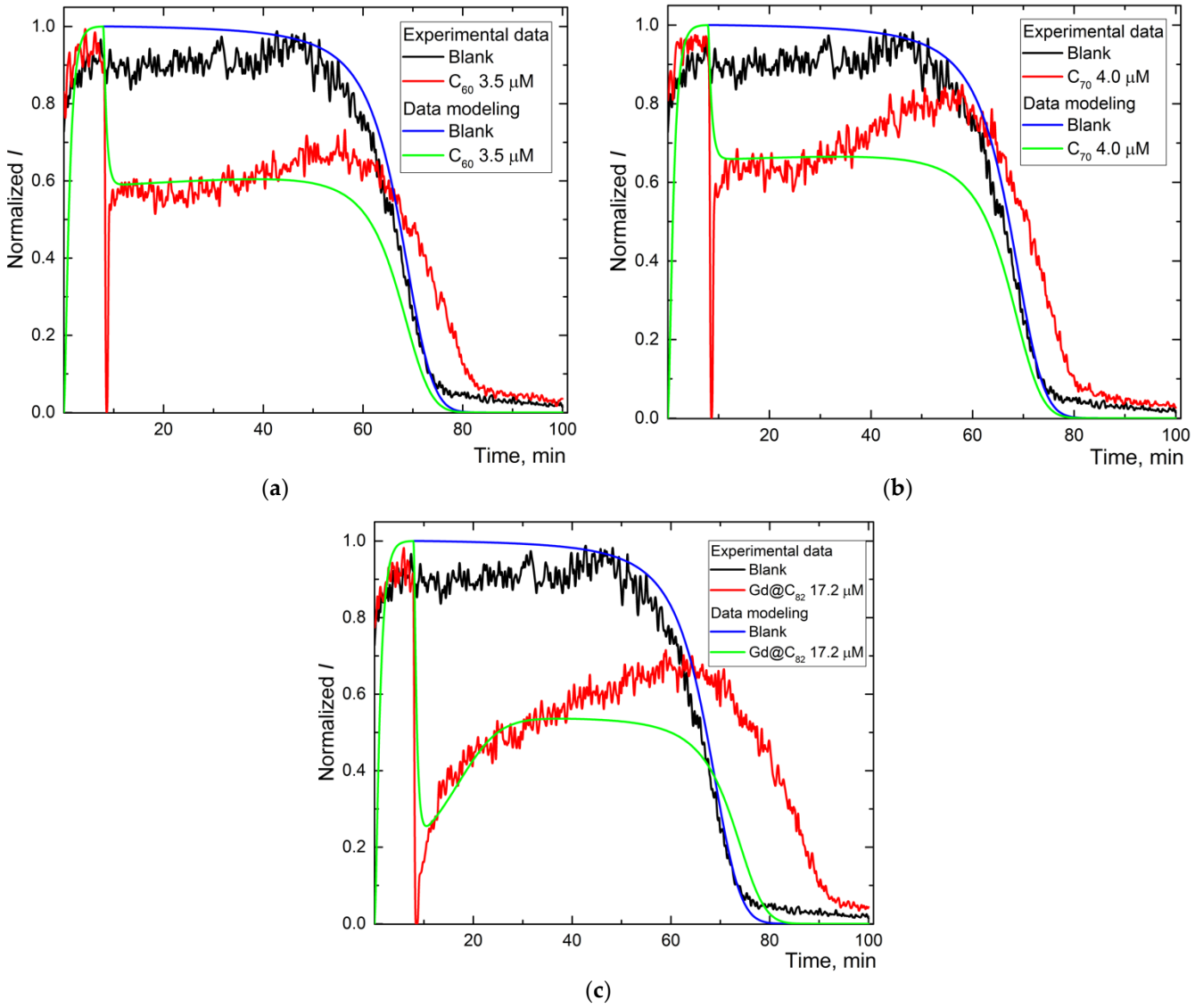

Figure 3. The experimental and simulated chemiluminescence plots for aqueous fullerene dispersions C_{60} (**a**), C_{70} (**b**), and Gd@C_{82} (**c**) for one-stage mechanism. Black is the blank; blue is the simulated data of the blank; red is experimental data for aqueous fullerene dispersions; and green is simulated data for aqueous fullerene dispersions.

Experimental and calculated plots have a sufficient degree of coincidence. For Trolox and AFDs, recording the whole curve required ca. 100 min (Figure 2b,d,f). The simulation shows the expected values of reactions (1), (2), and (2a) and the constant of the primary antioxidant process, the radical interception reaction (3) of 10^4 μM^{-1} min^{-1} (Table 2).

For AFDs, the rate constants of (1) and (2) differed insignificantly, while the rate constant of the luminescence process decreased by a factor of 4. Reaction (3a), the interaction of the antioxidant with the excited product of luminol was revealed for all AFDs; rates are in the order C_{60} > C_{70}~Gd@C_{82}, the ratio of reaction rate constants is 1.5:1:1. Along with a decrease in the rate constant of (2a), it can be considered quenching.

The reaction (3) intercepting radicals from ABAP is observed for Trolox and Gd@C_{82} AFD. The simulation shows that this process has a rate constant 300 times higher than the quenching (Table 2), while the concentration of the antioxidant calculated in the process (3) is estimated as 100 times lower than the total fullerene concentration in the AFD. The antioxidant activity of Gd@C_{82} is 300 times lower than for Trolox.

3. Discussion

The study [44] classified the antioxidant activity by rate constants as strong, higher than 2 μM^{-1} min^{-1}, medium, higher than 0.1 μM^{-1} min^{-1}, and weak, below 0.01 μM^{-1} min^{-1}. Strong oxidants can be measured easily; the medium can be measured, as well. In the case of weak oxidants, calibration is complicated as the action is weak and slow and probably does not return to the pre-application stationary CL level.

C_{60}, C_{70}, and Gd@C_{82} are comparable and refer to medium-strength antioxidants (Table 2). On the contrary, the same constants attributed to AO + RLum* reaction for C_{60}, C_{70}, and Gd@C_{82} reveal that fullerenes intercept the excited product of luminol. It is the quenching of chemiluminescence rather than competition with luminol molecules for free radicals, as the magnitude of the constant values shows (Table 2). Such a quenching mechanism and the role of fullerenes in reducing the fluorescence signal are still unclear [54]. In some cases, fullerenes and fullerenols can non-covalently bind molecules, e.g., Ribonuclease A [52] exhibiting static quenching. However, binding sites in each case are individual; for a more detailed study of the binding nature, molecular dynamics simulations should be performed [55]. We evaluated quenching for an ABAP–luminol mixture and luminol alone (see the Supporting information). In both cases, we observed comparable values of Stern–Volmer quenching constants for C_{60}, C_{70}, and Gd@C_{82} as C_{70} > C_{60} > Gd@C_{82}. This quenching can be explained by the average polarizability (α) of fullerene molecules. The polarizabilities as $\alpha_{EMF} < \alpha_{atom} + \alpha_{Fullerene}$ are 114.67 $Å^3$ for Gd@C_{82} [56], 102.7 $Å^3$ for C_{70} [57], and 82.7 $Å^3$ for C_{60}. Thus, the higher quenching efficiency of C_{70} and Gd@C_{82} can be attributed to its higher polarizability [58]. In addition, the reactivity upon A_E-type reactions for fullerenes decreased from C_{60} to Gd@C_{82} [59] as the presence of endoatoms improves the fullerene antiradical capacity [60]. A 1.3-fold decrease in the quenching constant for Gd@C_{82} could also be due to a different behavior in the chemiluminescence reaction, a change in the quenching mechanism to a bimolecular one [53] or another competing process at multiple positions of the fullerene cage [59].

From the data on antioxidant activity of AFDS of C_{60} and C_{70}, the following results can be summed up. AFDs of C_{60} and C_{70} show no pro-oxidant activity in the tested model; thus, they can be used for biomedical applications without any hazardous effect. In our opinion, low activity values and mainly quenching properties mean that AFDs of unmodified C_{60} and C_{70} can be used as control values for testing the antioxidant properties of fullerene derivatives. In such a case, any found activity can be attributed to the added functionality and not the fullerene cage.

The most relevant difference in antioxidant activity is that while C_{60} and C_{70} showed a single process that we attribute to quenching, a second process is revealed in Gd@C_{82}. This action in Gd@C_{82} is attributed to the interception of ABAP radicals, i.e., actual antioxidant activity. However, the significant CL quenching intrinsic to Gd@C_{82} as to other fullerenes makes it challenging to separate these two signals. This behavior for Gd@C_{82} AFD can be explained by the presence of a carbon cage containing the inner paramagnetic metal ion Gd^{3+} with a spin of 7/2 or Gd@$C_{82}{}^{3-}$ anion acting as a radical located on the outer shell [61]. Gd@$C_{82}{}^{3-}$ can be involved in free-radical addition reactions, which can change the electronic structure of the inner cluster and affect its configuration [62]. The electron affinity of Gd@C_{82} is more significant than those for pristine C_{60} and C_{70} (1.25 and 1.19 times, respectively$_2$). Gd@C_{82} acts as a strong electron donor and acceptor [63], which correlates with the relative efficiencies Gd@$C_{82}(OH)_{22}$ > $C_{60}(OH)_{22}$ to scavenge various free radicals [19]. It is noteworthy that the concentration of Gd@C_{82} was 4 times higher than C_{70} and C_{60} (17.2 and ~4 μM, respectively). Thus, the effect of the second process in Gd@C_{82} kinetics was more prominent. AFDs C_{60} and C_{70} may show the same antioxidant action, but it was less noticeable due to the concentrations.

Thus, for Gd@$C_{82,}$ we can conclude that it shows no pro-oxidant activity like AFDs of C_{60} and C_{70}, which is more relevant as Gd@C_{82} is considered for MRI applications [64]. Additionally, Gd@C_{82} shows medium antioxidant activity; thus, it can exhibit cytoprotective properties, which can be the topic of the subsequent study.

4. Materials and Methods

4.1. Aqueous Fullerene Dispersion Preparation

Preparation and characterization techniques for aqueous fullerene dispersions were recently described elsewhere [30]. In this work, we used long-term stable AFD of the pristine C_{60}, C_{70} (NeoTechProduct LLC (St. Petersburg, Russia), 99+% HPLC-grade); the enriched soot containing the Gd@C_{2n} EMFs (total content of Gd atoms up to 4 wt. % has been synthesized by the evaporation of the composite graphite electrodes compounded by gadolinium in the electric arc reactor as we previously described [65]. The sonication time was increased up to 36 h totally, and an ultrasound probe with a large surface was used (*ca*. 7 cm^2). The main drawback of this process is a time-dependent accumulation of titanium dioxide nanoparticles (TiO_2 NPs) due to cavitation sonotrode erosion. It is confirmed by ICP-OES analysis for metal impurities in AFDs (Table S1, Supplementary Materials).

A syringe hydrophilic polyvinylidene fluoride (PVDF) filter has been used to remove particles from AFDs. The filter removes large fullerene nanoparticles (more than 1 μm) and finally cleans out titanium nanoparticles (less than ca. 1 ppb) from the ultrasonic probe. ICP-OES showed that AFDs contain silicon, which cannot be removed by syringe filtering. The details on the aqueous fullerene dispersion preparation and material safety data sheet are summarized in the Supplementary Materials.

4.2. Techniques and Reagents

The enhanced chemiluminescence protocol for quantification of the antioxidant potential of AFD C_{60}, C_{70}, and Gd@C_{82} has been used. The chemiluminescent system consisted of a source of free radicals, cationic 2,2′-azobis (2-amidinopropane) dihydrochloride (ABAP; Sigma, St. Louis, MO, USA), and a chemiluminescent probe, 5-amino-2,3-dihydrophthalazine-1,4-dione. Reference antioxidant compound: Trolox® (±)-6-Hydroxy-2,5,7,8-tetra-methylchromane-2-carboxylic acid (Sigma, St. Louis, MO, USA).

A luminol solution of 1 mM (Sigma, USA) and ABAP solution of 50 mM were prepared by dissolving the weighed samples in a phosphate buffer solution 0.1 M KH_2PO_4 at pH 7.4 (Sigma, St. Louis, MO, USA). The total volume in a polycarbonate cuvette was 1.00 mL in all experiments. The stock solution of ABAP (2.5 mM) and luminol (2 μM) in the mixture were added to the buffer solution at 37 °C. Reagent addition order: (1) heated phosphate buffer solution, (2) mixture of ABAP and luminol incubated in the dark at room temperature for 20 min. After reaching a steady-state CL signal level, the AFDs, or Trolox® was added (shown as a sharp decrease in readout signal between 10 and 20 min, Figures 1 and 2). The CL signal was recorded until the new stationary level was reached.

The chemiluminescence signal was recorded up to achieving stationary level, and then an aliquot of the antioxidant solution of Trolox or AFDs was added. The registration was performed until the new steady-state level.

4.3. Equipment

The measurements were carried out with a Lum-1200 12-channel chemiluminometer (DISoft, Moscow, Russia). The chemiluminometer detects visible light in a range of 300–700 nm. No bandpass filters were used. Signal processing was performed via PowerGraph 3.3 Professional software (DISoft, Moscow, Russia). The relative standard deviation of chemiluminescence intensity did not exceed 0.05. Fluorolog®-2 spectrofluorimeter (Horiba Jobin Yvon, Kyoto, Japan) was used. An Agilent 720 ICP-OES spectrometer (Mulgrave, Australia) with an axial view was used for elemental analysis. The statistical processing of the data was performed with STATISTICA v.10.0 software (StatSoft Inc., Tulsa, OK, USA).

Millex-HV Syringe Filter Unit, 0.22 and 0.45 μm, hydrophilic PVDF, 33 mm, non-sterilized were used for AFD filtration during the preparation process (Merck Millipore, Darmstadt, Germany). Sartorius Proline Plus (Göttingen, Germany) mechanical single-channel pipettors of 10 ÷ 100, 100 ÷ 1000 μL were used for the graduation and preparation of solutions calibrated by ISO 8655-2:2002. The ultrasound probe MEF93.T (LLC MELFIZ-

ul'trazvuk, Moscow, Russia) working in a continuous mode of exposure to ultrasonic energy at operating frequency 22.00 ± 1.65 kHz has been used for AFD preparation. A SevenCompact™ pH/Ion S220 pH-meter (Mettler-Toledo AG, Greifensee, Switzerland) was used to prepare the phosphate buffer solution. According to IUPAC recommendation [66], calibration was performed using NIST Traceable standard buffer solutions with pH 1.68, 4.01, 6.68, 9.18, and 11.00 (Hanna Instruments, Woonsocket, RI, USA).

4.4. Computer Simulation and Data Handling

The computer simulation was carried out with the specially designed computer program Kinetic Analyzer (by Dr. D. Izmailov). For a set of the predetermined reactions and the initial concentrations of the reactants, the rate constants were selected, providing the maximal curve fitting of experimental and calculated plots. As a criterion for the best curve fitting, the minimum sum of squared residuals was calculated using OriginPro 2015 software (OriginLab Corp., Northampton, MA, USA).

We recorded the kinetics of chemiluminescence of antioxidant action to the moment of depletion of the antioxidant, ~100 min. The total areas and areas for the first 20 min of the reaction were calculated using the functional features of PowerGraph software. Chemiluminograms in the molecular model of generation of organic radicals were used to determine the concentration of half-suppression of the chemiluminescent signal for all AFDs ($c_{1/2}$, μM). The concentration of half-suppression of luminescence ($c_{1/2}$, μM) is a concentration that reduces the area the signal S of the response by two times and can hypothetically be taken as a quantitative indicator of the inhibitory activity of a given compound.

5. Conclusions

Thus, the antioxidant potential requires the estimation of both the thermodynamic and kinetic parts of this parameter. AFDs of C_{60} and C_{70} show no antioxidant activity in the system of organic radical-induced ABAP decay. We prove that it is not free radical capture but quenching. However, Gd@C_{82} has a dual-action mechanism involving a significant antioxidant action. The results provide insights into the possible mechanism of interactions of fullerenes between free-radicals C_{60}, C_{70}, Gd@C_{82}, which are fundamental to understanding the potential biomedical effects of AFDs. Evaluating the antioxidant activity of fullerenes is helpful in further evaluation of antioxidant properties in a living cell.

We believe that this work helps create reference materials for further study of the antioxidant properties of functional fullerene derivatives. AFDs of C_{60}, C_{70} can be proposed as model substances not exhibiting antioxidant properties. Moreover, the absence of a significant free radical interception effect allows the development of sensors to control impurity composition, acting as a free radical interceptor rather than as a quencher for in vitro and in vivo experiments.

Supplementary Materials: The following are available online at https://www.mdpi.com/article/10.3390/ijms22115838/s1, Figures S1 and S2, fluorescent spectra of aqueous fullerene dispersions C_{60}, C_{70}, and Gd@C_{82} act as a quencher at different systems ABAP-luminol, and only luminol. Table S1, the elemental composition of fullerene dispersions by inductively coupled plasma atomic emission spectroscopy (ICP-OES) and pH measurements.

Author Contributions: Conceptualization, E.V.P. and M.A.P.; methodology, E.V.P. and M.A.P.; software, D.Y.I.; validation, I.V.M. and M.M.S.; formal analysis, I.V.M., M.M.S. and D.Y.I.; investigation, I.V.M. and M.M.S.; resources, I.E.K.; data curation, I.V.M. and E.V.P.; writing—original draft preparation, I.V.M.; writing—review and editing, E.V.P. and M.A.P.; supervision, E.V.P. and M.A.P.; project administration, M.A.P.; funding acquisition, I.V.M. All authors have read and agreed to the published version of the manuscript.

Funding: The Russian Science Foundation has supported this work under Contract No. 19-73-00143. This research was performed according to the Development program of the Interdisciplinary Scientific

and Educational School of Lomonosov Moscow State University, "The future of the planet and global environmental change".

Institutional Review Board Statement: Not applicable.

Informed Consent Statement: Not applicable.

Data Availability Statement: Raw data and samples of the aqueous dispersions of fullerenes and endofullerene compounds are available from the authors.

Acknowledgments: V.P. Bubnov provided the technical support for Gd–endofullerene synthesis.

Conflicts of Interest: The authors declare no conflict of interest.

References

1. Colvin, V.L. The potential environmental impact of engineered nanomaterials. *Nat. Biotechnol.* **2003**, *21*, 1166–1170. [CrossRef] [PubMed]
2. Chi, Y.; Bhonsle, J.B.; Canteenwala, T.; Huang, J.-P.; Shiea, J.; Chen, B.-J.; Chiang, L.Y. Novel Water-soluble Hexa(sulfobutyl)fullerenes as Potent Free Radical Scavengers. *Chem. Lett.* **1998**, *27*, 465–466. [CrossRef]
3. Witte, P.; Beuerle, F.; Hartnagel, U.; Lebovitz, R.; Savouchkina, A.; Sali, S.; Guldi, D.; Chronakis, N.; Hirsch, A. Water solubility, antioxidant activity and cytochrome C binding of four families of exohedral adducts of C_{60} and C_{70}. *Org. Biomol. Chem.* **2007**, *5*, 3599–3613. [CrossRef]
4. Pellarini, F.; Pantarotto, D.; Da Ros, T.; Giangaspero, A.; Tossi, A.; Prato, M. A Novel [60]Fullerene Amino Acid for Use in Solid-Phase Peptide Synthesis. *Org. Lett.* **2001**, *3*, 1845–1848. [CrossRef]
5. Cheng, F.; Yang, X.; Fan, C.; Zhu, H. Organophosphorus chemistry of fullerene: Synthesis and biological effects of organophosphorus compounds of C_{60}. *Tetrahedron* **2001**, *57*, 7331–7335. [CrossRef]
6. Kamat, J.P.; Devasagayam, T.P.; Priyadarsini, K.I.; Mohan, H. Reactive oxygen species mediated membrane damage induced by fullerene derivatives and its possible biological implications. *Toxicology* **2000**, *155*, 55–61. [CrossRef]
7. Andrievsky, G.V.; Kosevich, M.V.; Vovk, O.M.; Shelkovsky, V.S.; Vashchenko, L.A. On the production of an aqueous colloidal solution of fullerenes. *J. Chem. Soc. Chem. Commun.* **1995**, 1281–1282. [CrossRef]
8. Andreev, S.; Purgina, D.; Bashkatova, E.; Garshev, A.; Maerle, A.; Andreev, I.; Osipova, N.; Shershakova, N.; Khaitov, M. Study of Fullerene Aqueous Dispersion Prepared by Novel Dialysis Method: Simple Way to Fullerene Aqueous Solution. *Fuller. Nanotub. Carbon Nanostruct.* **2014**, *23*, 792–800. [CrossRef]
9. Isaacson, C.W.; Bouchard, D. Asymmetric flow field flow fractionation of aqueous C_{60} nanoparticles with size determination by dynamic light scattering and quantification by liquid chromatography atmospheric pressure photo-ionization mass spectrometry. *J. Chromatogr. A* **2010**, *1217*, 1506–1512. [CrossRef] [PubMed]
10. Prylutskyy, Y.I.; Petrenko, V.I.; Ivankov, O.I.; Kyzyma, O.A.; Bulavin, L.A.; Litsis, O.O.; Evstigneev, M.P.; Cherepanov, V.V.; Naumovets, A.G.; Ritter, U. On the Origin of C_{60} Fullerene Solubility in Aqueous Solution. *Langmuir* **2014**, *30*, 3967–3970. [CrossRef]
11. Pycke, B.F.G.; Halden, R.U.; Benn, T.M.; Westerhoff, P.; Herckes, P. Strategies for quantifying C_{60} fullerenes in environmental and biological samples and implications for studies in environmental health and ecotoxicology. *TrAC Trends Anal. Chem.* **2011**, *30*, 44–57. [CrossRef]
12. Nel, A.E.; Mädler, L.; Velegol, D.; Xia, T.; Hoek, E.M.V.; Somasundaran, P.; Klaessig, F.; Castranova, V.; Thompson, M. Understanding biophysicochemical interactions at the nano-bio interface. *Nat. Mater.* **2009**, *8*, 543–557. [CrossRef] [PubMed]
13. Johnston, H.J.; Hutchison, G.R.; Christensen, F.M.; Aschberger, K.; Stone, V. The Biological Mechanisms and Physicochemical Characteristics Responsible for Driving Fullerene Toxicity. *Toxicol. Sci.* **2009**, *114*, 162–182. [CrossRef] [PubMed]
14. Sharoyko, V.V.; Ageev, S.V.; Podolsky, N.E.; Petrov, A.V.; Litasova, E.V.; Vlasov, T.D.; Vasina, L.V.; Murin, I.V.; Piotrovskiy, L.B.; Semenov, K.N. Biologically active water-soluble fullerene adducts: Das Glasperlenspiel (by H. Hesse)? *J. Mol. Liq.* **2021**, *323*, 114990. [CrossRef]
15. Valgimigli, L.; Baschieri, A.; Amorati, R. Antioxidant activity of nanomaterials. *J. Mater. Chem. B* **2018**, *6*, 2036–2051. [CrossRef]
16. Enes, R.F.; Tomé, A.C.; Cavaleiro, J.A.S.; Amorati, R.; Fumo, M.G.; Pedulli, G.F.; Valgimigli, L. Synthesis and Antioxidant Activity of [60]Fullerene–BHT Conjugates. *Chem. Eur. J.* **2006**, *12*, 4646–4653. [CrossRef]
17. Czochara, R.; Kusio, J.; Litwinienko, G. Fullerene C_{60} conjugated with phenols as new hybrid antioxidants to improve the oxidative stability of polymers at elevated temperatures. *RSC Adv.* **2017**, *7*, 44021–44025. [CrossRef]
18. Czochara, R.; Grajda, M.; Kusio, J.; Litwinienko, G. Expanding the antioxidant activity into higher temperatures—Fullerene C_{60} conjugated with α-Tocopherol analogue as a hybrid antioxidant in saturated lipid systems. *Bulg. Chem. Commun.* **2018**, *50*, 268–274.
19. Yin, J.-J.; Lao, F.; Fu, P.P.; Wamer, W.G.; Zhao, Y.; Wang, P.C.; Qiu, Y.; Sun, B.; Xing, G.; Dong, J.; et al. The scavenging of reactive oxygen species and the potential for cell protection by functionalized fullerene materials. *Biomaterials* **2009**, *30*, 611–621. [CrossRef] [PubMed]

20. Sachkova, A.S.; Kovel, E.S.; Churilov, G.N.; Guseynov, O.A.; Bondar, A.A.; Dubinina, I.A.; Kudryasheva, N.S. On mechanism of antioxidant effect of fullerenols. *Biochem. Biophys. Rep.* **2017**, *9*, 1–8. [CrossRef]
21. Kovel, E.S.; Sachkova, A.S.; Vnukova, N.G.; Churilov, G.N.; Knyazeva, E.M.; Kudryasheva, N.S. Antioxidant Activity and Toxicity of Fullerenols via Bioluminescence Signaling: Role of Oxygen Substituents. *Int. J. Mol. Sci.* **2019**, *20*, 2324. [CrossRef]
22. Eropkin, M.Y.; Melenevskaya, E.Y.; Nasonova, K.V.; Bryazzhikova, T.S.; Eropkina, E.M.; Danilenko, D.M.; Kiselev, O.I. Synthesis and Biological Activity of Fullerenols with Various Contents of Hydroxyl Groups. *Pharm. Chem. J.* **2013**, *47*, 87–91. [CrossRef]
23. Zhou, S.; Yamamoto, M.; Briggs, G.A.D.; Imahori, H.; Porfyrakis, K. Probing the Dipolar Coupling in a Heterospin Endohedral Fullerene–Phthalocyanine Dyad. *J. Am. Chem. Soc.* **2016**, *138*, 1313–1319. [CrossRef]
24. Hamblin, M.R. Fullerenes as photosensitizers in photodynamic therapy: Pros and cons. *Photochem. Photobiol. Sci.* **2018**, *17*, 1515–1533. [CrossRef] [PubMed]
25. Tzirakis, M.D.; Orfanopoulos, M. Radical Reactions of Fullerenes: From Synthetic Organic Chemistry to Materials Science and Biology. *Chem. Rev.* **2013**, *113*, 5262–5321. [CrossRef]
26. Mikheev, I.V.; Sozarukova, M.M.; Proskurnina, E.V.; Kareev, I.E.; Proskurnin, M.A. Non-Functionalized Fullerenes and Endofullerenes in Aqueous Dispersions as Superoxide Scavengers. *Molecules* **2020**, *25*, 2506. [CrossRef]
27. Grebowski, J.; Konopko, A.; Krokosz, A.; DiLabio, G.A.; Litwinienko, G. Antioxidant activity of highly hydroxylated fullerene C_{60} and its interactions with the analogue of α-tocopherol. *Free Radic. Biol. Med.* **2020**, *160*, 734–744. [CrossRef] [PubMed]
28. Shinohara, N.; Matsumoto, T.; Gamo, M.; Miyauchi, A.; Endo, S.; Yonezawa, Y.; Nakanishi, J. Is Lipid Peroxidation Induced by the Aqueous Suspension of Fullerene C_{60} Nanoparticles in the Brains of *Cyprinus carpio*? *Environ. Sci. Technol.* **2008**, *43*, 948–953. [CrossRef] [PubMed]
29. Prylutska, S.V.; Grynyuk, I.I.; Matyshevska, O.P.; Prylutskyy, Y.I.; Ritter, U.; Scharff, P. Anti-oxidant Properties of C_{60} Fullerenes in vitro. *Fuller. Nanotub. Carbon Nanostruct.* **2008**, *16*, 698–705. [CrossRef]
30. Mikheev, I.V.; Pirogova, M.O.; Usoltseva, L.O.; Uzhel, A.S.; Bolotnik, T.A.; Kareev, I.E.; Bubnov, V.P.; Lukonina, N.S.; Volkov, D.S.; Goryunkov, A.A.; et al. Green and rapid preparation of long-term stable aqueous dispersions of fullerenes and endohedral fullerenes: The pros and cons of an ultrasonic probe. *Ultrason. Sonochem.* **2021**, *73*, 105533. [CrossRef] [PubMed]
31. Wang, C.; Lin, Y.; Wang, Y.; Liang, Y.; Meng, L.; Zhang, J.; Zhou, Q.; Jiang, G. Induced temperature-dependent DNA degradation by C_{60} without photoactivation. *Chin. Sci. Bull.* **2011**, *56*, 3100–3107. [CrossRef]
32. Wang, I.C.; Tai, L.A.; Lee, D.D.; Kanakamma, P.P.; Shen, C.K.-F.; Luh, T.-Y.; Cheng, C.H.; Hwang, K.C. C_{60} and Water-Soluble Fullerene Derivatives as Antioxidants against Radical-Initiated Lipid Peroxidation. *J. Med. Chem.* **1999**, *42*, 4614–4620. [CrossRef] [PubMed]
33. Skulachev, M.V.; Antonenko, Y.N.; Anisimov, V.N.; Chernyak, B.V.; Cherepanov, D.A.; Chistyakov, V.A.; Egorov, M.V.; Kolosova, N.G.; Korshunova, G.A.; Lyamzaev, K.G.; et al. Mitochondrial-Targeted Plastoquinone Derivatives. Effect on Senescence and Acute Age-Related Pathologies. *Curr. Drug Targets* **2011**, *12*, 800–826. [CrossRef]
34. Chistyakov, V.A.; Smirnova, Y.O.; Prazdnova, E.V.; Soldatov, A.V. Possible Mechanisms of Fullerene C_{60} Antioxidant Action. *BioMed Res. Int.* **2013**, *2013*, 821498. [CrossRef]
35. Prylutska, S.V.; Matyshevska, O.P.; Grynyuk, I.I.; Prylutskyy, Y.I.; Ritter, U.; Scharff, P. Biological Effects of C_{60} Fullerenes in vitro and in a Model System. *Mol. Cryst. Liq. Cryst.* **2007**, *468*, 265/[617]–274/[626]. [CrossRef]
36. Zeynalov, E.B.; Allen, N.S.; Salmanova, N.I. Radical scavenging efficiency of different fullerenes C_{60}–C_{70} and fullerene soot. *Polym. Degrad. Stab.* **2009**, *94*, 1183–1189. [CrossRef]
37. Bulgakov, R.G.; Ponomareva, Y.G.; Maslennikov, S.I.; Nevyadovsky, E.Y.; Antipina, S.V. Inertness of C_{60} fullerene toward $RO_2^{\bullet}$ peroxy radicals. *Russ. Chem. Bull.* **2005**, *54*, 1862–1865. [CrossRef]
38. Lissi, E.; Salim-Hanna, M.; Pascual, C.; del Castillo, M.D. Evaluation of total antioxidant potential (TRAP) and total antioxidant reactivity from luminol-enhanced chemiluminescence measurements. *Free Radic. Biol. Med.* **1995**, *18*, 153–158. [CrossRef]
39. Magin, D.V.; Izmaĭlov, D.I.; Popov, I.N.; Levin, G.; Vladimirov, I.A. Photochemiluminescent study of the antioxidant activity in biological systems. Mathematical modeling. *Vopr. Med. Khimii* **2000**, *46*, 419–425.
40. Vladimirov, Y.A.; Proskurnina, E.V.; Izmajlov, D.Y. Kinetic chemiluminescence as a method for study of free radical reactions. *Biophysics* **2011**, *56*, 1055–1062. [CrossRef]
41. Sozarukova, M.M.; Shestakova, M.A.; Teplonogova, M.A.; Izmailov, D.Y.; Proskurnina, E.V.; Ivanov, V.K. Quantification of Free Radical Scavenging Properties and SOD-Like Activity of Cerium Dioxide Nanoparticles in Biochemical Models. *Russ. J. Inorg. Chem.* **2020**, *65*, 597–605. [CrossRef]
42. Brainina, K.; Stozhko, N.; Vidrevich, M. Antioxidants: Terminology, Methods, and Future Considerations. *Antioxidants* **2019**, *8*, 297. [CrossRef] [PubMed]
43. Apak, R.; Gorinstein, S.; Böhm, V.; Schaich, K.M.; Özyürek, M.; Güçlü, K. Methods of measurement and evaluation of natural antioxidant capacity/activity (IUPAC Technical Report). *Pure Appl. Chem.* **2013**, *85*, 957–998. [CrossRef]
44. Proskurnina, E.V.; Izmailov, D.Y.; Sozarukova, M.M.; Zhuravleva, T.A.; Leneva, I.A.; Poromov, A.A. Antioxidant Potential of Antiviral Drug Umifenovir. *Molecules* **2020**, *25*, 1577. [CrossRef]
45. Boulebd, H. Comparative study of the radical scavenging behavior of ascorbic acid, BHT, BHA and Trolox: Experimental and theoretical study. *J. Mol. Struct.* **2020**, *1201*, 127210. [CrossRef]
46. Lissi, E.; Pascual, C.; Del Castillo, M.D. Luminol Luminescence Induced by 2,2′-Azo-Bis(2-Amidinopropane) Thermolysis. *Free Radic. Res. Commun.* **1992**, *17*, 299–311. [CrossRef] [PubMed]

47. Jian, C.; Yan, J.; Zhang, H.; Zhu, J. Recent advances of small molecule fluorescent probes for distinguishing monoamine oxidase-A and monoamine oxidase-B in vitro and in vivo. *Mol. Cell. Probes* **2021**, *55*, 101686. [CrossRef] [PubMed]
48. Gharbi, N.; Pressac, M.; Hadchouel, M.; Szwarc, H.; Wilson, S.R.; Moussa, F. [60]Fullerene is a Powerful Antioxidant In Vivo with No Acute or Subacute Toxicity. *Nano Lett.* **2005**, *5*, 2578–2585. [CrossRef]
49. Catalan, J.; Elguero, J. Fluorescence of fullerenes (C_{60} and C_{70}). *J. Am. Chem. Soc.* **1993**, *115*, 9249–9252. [CrossRef]
50. Campbell, K.; Zappas, A.; Bunz, U.; Thio, Y.S.; Bucknall, D.G. Fluorescence quenching of a poly(para-phenylene ethynylenes) by C_{60} fullerenes. *J. Photochem. Photobiol. A Chem.* **2012**, *249*, 41–46. [CrossRef]
51. Liu, B.-M.; Zhang, J.; Hao, A.-J.; Xu, L.; Wang, D.; Ji, H.; Sun, S.-J.; Chen, B.-Q.; Liu, B. The increased binding affinity of curcumin with human serum albumin in the presence of rutin and baicalin: A potential for drug delivery system. *Spectrochim. Acta Mol. Biomol. Spectrosc.* **2016**, *155*, 88–94. [CrossRef] [PubMed]
52. Roy, P.; Bag, S.; Chakraborty, D.; Dasgupta, S. Exploring the Inhibitory and Antioxidant Effects of Fullerene and Fullerenol on Ribonuclease A. *ACS Omega* **2018**, *3*, 12270–12283. [CrossRef]
53. Liu, X.; Ying, X.; Li, Y.; Yang, H.; Hao, W.; Yu, M. Identification differential behavior of Gd@C_{82}(OH)$_{22}$ upon interaction with serum albumin using spectroscopic analysis. *Spectrochim. Acta Mol. Biomol. Spectrosc.* **2018**, *203*, 383–396. [CrossRef]
54. Sluch, M.; Samuel, I.; Petty, M. Quenching of pyrene fluorescence by fullerene C_{60} in Langmuir–Blodgett films. *Chem. Phys. Lett.* **1997**, *280*, 315–320. [CrossRef]
55. Mchedlov-Petrossyan, N.O. Fullerenes in Liquid Media: An Unsettling Intrusion into the Solution Chemistry. *Chem. Rev.* **2013**, *113*, 5149–5193. [CrossRef] [PubMed]
56. Zakharova, A.V.; Bedrina, M.E. A quantum chemical study of endometallofullerenes: Gd@C_{70}, Gd@C_{82}, Gd@C_{84}, and Gd@C_{90}. *Eur. Phys. J. D* **2020**, *74*, 116. [CrossRef]
57. Compagnon, I.; Antoine, R.; Broyer, M.; Dugourd, P.; Lermé, J.; Rayane, D. Electric polarizability of isolated C_{70} molecules. *Phys. Rev. A* **2001**, *64*, 025201. [CrossRef]
58. Bulgakov, R.G.; Galimov, D.I.; Sabirov, D.S. New property of the fullerenes: The anomalously effective quenching of electronically excited states owing to energy transfer to the C_{70} and C_{60} molecules. *JETP Lett.* **2007**, *85*, 632–635. [CrossRef]
59. Wang, Z.; Lu, Z.-H.; Zhao, Y.; Gao, X. Oxidation-induced water-solubilization and chemical functionalization of fullerenes C_{60}, Gd@C_{60} and Gd@C_{82}: Atomistic insights into the formation mechanisms and structures of fullerenols synthesized by different methods. *Nanoscale* **2015**, *7*, 2914–2925. [CrossRef]
60. Andrade, E.-B.; Martínez, A. Free radical scavenger properties of metal-fullerenes: C_{60} and C_{82} with Cu, Ag and Au (atoms and tetramers). *Comput. Theor. Chem.* **2017**, *1115*, 127–135. [CrossRef]
61. Furukawa, K.; Okubo, S.; Kato, H.; Shinohara, H.; Kato, T. High-Field/High-Frequency ESR Study of Gd@C_{82}-I. *J. Phys. Chem. A* **2003**, *107*, 10933–10937. [CrossRef]
62. Fang, H.; Cong, H.; Suzuki, M.; Bao, L.; Yu, B.; Xie, Y.; Mizorogi, N.; Olmstead, M.M.; Balch, A.L.; Nagase, S.; et al. Regioselective Benzyl Radical Addition to an Open-Shell Cluster Metallofullerene. Crystallographic Studies of Cocrystallized Sc_3C_2@Ih-C_{80} and Its Singly Bonded Derivative. *J. Am. Chem. Soc.* **2014**, *136*, 10534–10540. [CrossRef] [PubMed]
63. Guha, S.; Nakamoto, K. Electronic structures and spectral properties of endohedral fullerenes. *Coord. Chem. Rev.* **2005**, *249*, 1111–1132. [CrossRef]
64. Ghiassi, K.B.; Olmstead, M.M.; Balch, A.L. Gadolinium-containing endohedral fullerenes: Structures and function as magnetic resonance imaging (MRI) agents. *Dalton Trans.* **2014**, *43*, 7346–7358. [CrossRef]
65. Bubnov, V.P.; Laukhina, E.E.; Kareev, I.E.; Koltover, V.K.; Prokhorova, T.G.; Yagubskii, E.B.; Kozmin, Y.P. Endohedral Metallofullerenes: A Convenient Gram-Scale Preparation. *Chem. Mater.* **2002**, *14*, 1004–1008. [CrossRef]
66. Buck, R.P.; Rondinini, S.; Covington, A.K.; Baucke, F.G.K.; Brett, C.M.A.; Camoes, M.F.; Milton, M.J.T.; Mussini, T.; Naumann, R.; Pratt, K.W.; et al. Measurement of pH. Definition, standards, and procedures (IUPAC Recommendations 2002). *Pure Appl. Chem.* **2002**, *74*, 2169–2200. [CrossRef]